The effect of selective laser melting build orientation on the mechanical properties of AlSi10Mg parts

IOP Conf. Series: Materials Science and Engineering **430** (2018) 012028 doi:10.1088/1757-899X/430/1/012028

The effect of selective laser melting build orientation on the mechanical properties of AlSi10Mg parts

B J Mfusi[1,2,*], L C Tshabalala[2], A P I Popoola[1] and N R Mathe[2,*]

[1] Tshwane University of Technology, Department of Mechanical and Metallurgical Engineering, Staatsartillerie Rd, Pretoria West, Pretoria, 0183, South Africa
[2] National Laser Centre, Council for Scientific and Industrial Research, Meiring Naudé Road, Brummeria, Pretoria, 0185, South Africa

[*]mfusibusisiwe08@gmail.com, nmathe@csir.co.za

Abstract. Additive manufacturing is currently applied across a broad material selection and it is growing in production volume and economic impact. Aluminium is one of the materials that play a significant role in the aerospace industry because of its good strength-to-weight ratio. However, comparatively lower interest is shown in the additive manufacturing of aluminium alloys compared to titanium alloys, therefore there is much scope for data gathering and development of this material. In this investigation, the microstructure and mechanical properties of AlSi10Mg that were built using selective laser melting at different orientations are explored. The specimen were built in the XY, 45º and Z orientations. The microstructures of the obtained samples showed typical scan patterns with the density and hardness values similar to literature values. The XY built samples showed the lowest level of porosity and also possessed the lowest ultimate tensile strength and elongation. In contrast, the 45° built samples showed the highest ductility with the Z build samples showing the highest ultimate tensile strength. This behaviour is anisotropic where different properties are observed for different build orientations, thus the build orientation should be taken into consideration during the optimization of the laser processing parameters.

1. Introduction

Selective laser melting (SLM) is a process that uses a laser beam to build up a part by melting metal powder layer on top of a layer from computer-aided design data [1]. The core parameters that affect the built part includes; laser power, powder layer thickness, layer overlap and the scanning speed [2]. Various materials are used for additive manufacturing (AM) and aluminium (Al) alloys are increasingly becoming desirable in the aircraft and railway transportation industry according to Li et al., [3], which could increase the applications of SLM Al produced parts. In the limited amount of literature reviewed, there are numerous difficulties encountered regarding the success of SLM processing of aluminium based alloys, which are the high thermal conductivity and reflectivity. These properties lead to a need for intensified laser power essential for melting with the drawback being the oxidation of the alloys which leads to entrapment of oxide inclusions causing weak spots inside the parts [1]. Therefore, it is important to optimize the SLM processing parameters in order to obtain the optimum mechanical properties and porosity levels of less than 0.05% for as-built parts as required in the aerospace industry [4]. The other aspect of SLM that is deem crucial is the build orientation. It has

been determined that the build orientation affects the various properties such as porosity and mechanical properties as different microstructures are obtained based on the selected build orientation.

Therefore, this study aims to investigate the effect of build orientation on the mechanical properties of SLM produced AlSi10Mg before heat treatment or stress relieving. The samples were built in three different orientation of XY horizontal, 45º diagonal and Z vertical. These samples will be examined for various properties such as hardness, part density, porosity, microstructural changes and mechanical properties in order to determine the orientation that can be better modified and give ideal properties that are desirable for industrial use. All the samples were produced using fixed laser processing parameters.

2. Experimental Procedure

The tensile samples presented in figure 1 were built using the SLM Solutions M280, which is a commercial system with fixed parameters of; 150W power, 1000 mm/s scan speed, 50 µm hatch spacing and 50 µm powder layer thickness. A set of four samples per orientation were produced, with tensile testing performed using 3 of the samples and the remaining sample was sectioned for microstructural characterization. The samples are denoted as: XY (batch A), 45° (batch B) and Z (batch C) as seen in figure 1.

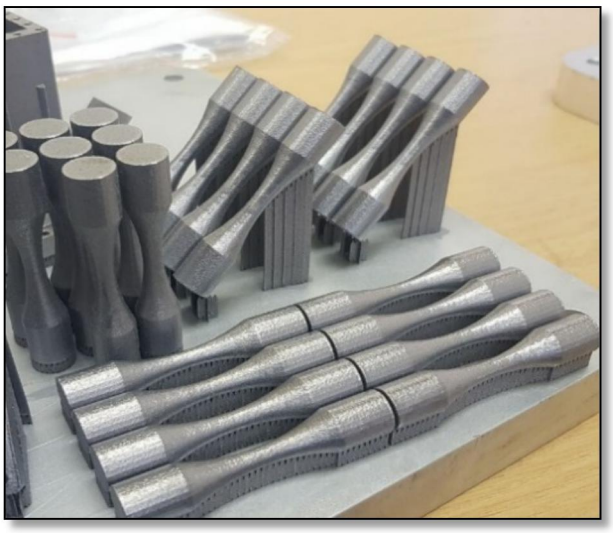

Figure 1*:* SLM produced AlSi10Mg samples in different build orientations.

2.1. Characterization.

Density measurements were performed on the tensile specimens using the OHAUS EX244/AD densitometers applying the Archimedes method in ethanol. The samples were sectioned, mounted, polished and etched using Keller's reagent prior to microstructural characterisation with the Olympus BX51M light optical microscope. The mounted specimen were also characterized for hardness on the Zwick Micro/Macro Vickers hardness tester. The load used in this case was 300 g and 20 indents were taken and averaged per sample. The 20kN Zwick/ Roell Tensile tester was used applying standard ASTM E8/E8M-16a for tensile strength measurements.

3. Results

3.1. Density and porosity measurements

The density and porosity results of the SLM built AlSi10Mg parts using different build orientations are presented in table 1. The densities obtained for the different orientations were similar and in agreement with the literature value of 2.67 g/cm^3 obtained for commercially produced AlSi10Mg samples [5]. In these results, it was observed that for all the build orientations, batch A (XY orientation) showed less porosity than the rest of the orientations, thus having a higher relative density. Whereas the highest amount of porosity was observed on batch C (Z orientation). The porosity levels obtained in these samples was less than the 0.15% with a relative density of above 99.8% as required for as-built samples for applications in the aerospace industry [4, 6]. To improve the porosity levels post heat treatments are performed on the samples but this will not be addressed in this work. The hardness measurements were also similar and will be discussed further in section 3.3.

Table 1: Properties of SLM produced sample in different orientations

Build orientations	Density (g/cm^3)	%Porosity	Relative density	Hardness (Hv)
A (XY)	2.679 ± 0.0133	0.037 ± 0.00019	99.96 ± 0.50	127 ± 0.635
B (45°)	2.677 ± 0.0132	0.112 ± 0.00056	99.88 ± 0.51	128 ± 0.641
C (Z)	2.676 ± 0.0014	0.149 ± 0.00075	99.85 ± 0.50	126 ± 0.630

For clarity on the porosity results observed in table 1, the microstructures of the samples were analysed to determine the presence of pores on the internal surfaces of the samples.

3.2 Microstructural analysis

The scanning direction microstructures of the SLM samples produced in different orientations are presented in figure 2. The images of batch A at different magnifications (figure 2a&d), show a microstructure consistent with the laser scan pattern during SLM process. This scale-like morphology was also observed by Rosenthal et al, [1]. The scanning pattern sizes in figure 2a were measured using Image J and they were; 50 – 90 µm height and 120 – 330 µm width and at higher magnifications, figure 2d, shows the presence of cellular and dendrite growth within the grain. The same was observed by Brandl et al., [6], Rosenthal et al., [7], and Lam et al., [8], which they attributed to the eutectic silicon particles within the grain boundaries.

The pores (black spots on the microstructure) of this sample were scattered and they were not observed in all tracks. For their work on SLM processed AlSi10Mg samples, Kempen et al. [9], and Awd et al., [10], also observed different types of pores, which are irregular and located at the melt pool boundaries, resulting from entrapped gasses as oxides or evaporated powder.

The microstructures of batch B samples (figure 2b&d), also showed a laser scan pattern though in this case the grains were diagonal to the laser scan path. The scan pattern sizes were also measured as height; 28 – 156 µm, and width; 113 – 344 µm and there were pores observed on every track including grain boundaries. Figure 2b&e showed the growth of dendrites on the boundaries and cellular growth which is larger than the dendrite growth in the middle of the structural morphology. Lam et al., [8], mentioned that the dendritic growth was supressed as a result of experiencing high solidification rate. A scale pattern similar to that of batch A was also observed in figure 2c&f, batch C. The scan pattern sizes were measured as height; 50 – 135 µm and width; 140 – 248 µm. There were pores observed in this structure especially on figure 2c. These pores could be as a result of undissolved powder or insufficient overlapping between scan tracks and spherical pores are usually as a result of trapped gasses, which might be oxides or evaporated powder. The pores are located within the melt pools which was also observed by Kempen et al., [11]. The levels of porosity observed in the microstructures are in agreement with measured porosity from Archimedes method presented in table

1, where the Z orientation possessed the highest quantified porosity and visible pores on the microstructures.

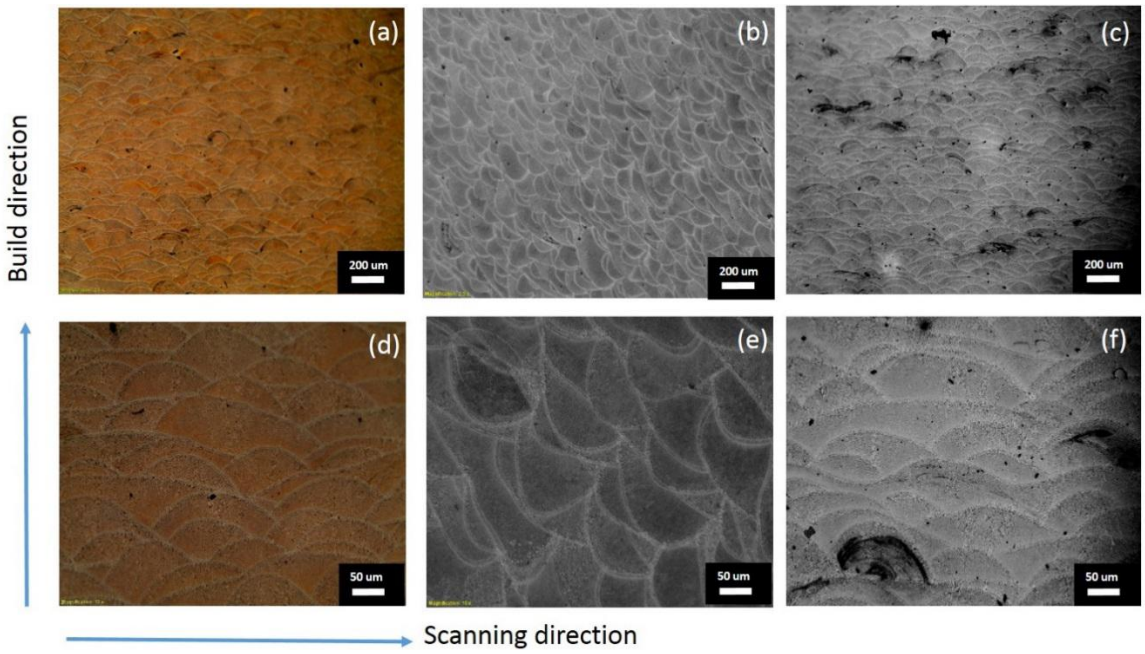

Figure 2. Microstructure of the SLM produced AlSi10Mg samples in various orientations, (a&d) XY, (b&e) 45°, and (c&f) Z orientations. (Images are in low and high magnification respectively.

3.3. Mechanical properties analysis

The hardness measurements are presented in table 1, where the values obtained varied from 126 – 128 Hv, which were relatively higher than values of 92 ± 5 Hv obtained by Rosenthal et al, [12], for SLM produced parts. The values were similar and showed little variations with the change in build orientation. Tensile tests were performed on the samples as shown in figure 3 in order to determine the effect of build orientation on the mechanical properties of the built parts. Typical stress-strain curves were obtained for the samples.

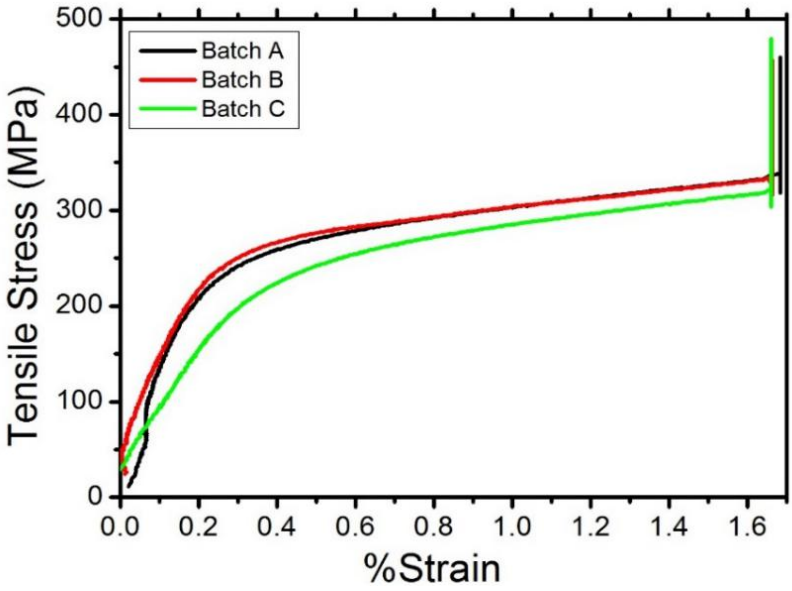

Figure 3. Stress-strain curves of the SLM produced AlSi10Mg samples with build orientation.

The modulus of elasticity for batch A was 83.5 MPa, which was above the expected elasticity of AlSi10Mg of 70 MPa [12]. The elasticity was only endured up to 2.4 mm extension; withstanding stress of up to less than 264 MPa and breaking at 5 mm at stress below 460 MPa. The modulus of elasticity of batch B was 82 MPa, which was also higher than obtained in literature. The elasticity in this case was endured up to 3.8 mm extension; withstanding stress of up to less than 268 MPa and breaking below 7 mm at stress below 462 MPa. This was due to the large number of pores as explained by Takata et al., [13], that SLM produced porous Al alloys exhibit an unstable compressive stress nature characterized by the peaks and troughs. The modulus of elasticity of batch C was 71 MPa, which was almost equal to the expected elasticity of AlSi10Mg of 70 MPa. The elasticity was only endured up to 2 mm extension; withstanding stress of up to less than 244 MPa and actually breaks below 5mm at stress below 473 MPa.

The average ultimate tensile strength (UTS) values of triplicate measurements derived from the stress-strain curves are presented in figure 4a plotted against the build orientation. The highest UTS was obtained for batch C at 473 ± 6 MPa, with batch A showing the lowest UTS value of 460 ± 4 MPa. The values obtained were in the same UTS range for selective laser sintering (460 MPa) [14], and higher than values obtained by Rosenthal et al., [12], for SLM produced AlSi10Mg after stress relieving (272 MPa), and Calagno et al.,[15], for casted A357 alloy (388 MPa). Figure 4b shows the plot of elongation against build orientation. Batch B possessed the highest elongation at 7.4%, and batch A showed the lowest elongation at 6.3%. However, these elongations are lower than the stress relieved AlSi10Mg SLM samples produced by Rosenthal et al.,(8.5%), [12], and they are comparable to the heat treated AlSi10Mg SLS data (6 – 9%), [15], and higher than the elongations for die-casted Aluminium A357 alloy (5.3%). The trend obtained for the samples in this case contradicts what was obtained in literature for the SLS where the Z-orientation samples showed lower elongation compared to XY-orientation and the SLM where the Z-orientation showed the highest elongation [5]. In this case, the highest ductility was obtained in batch B which is the 45° build orientation.

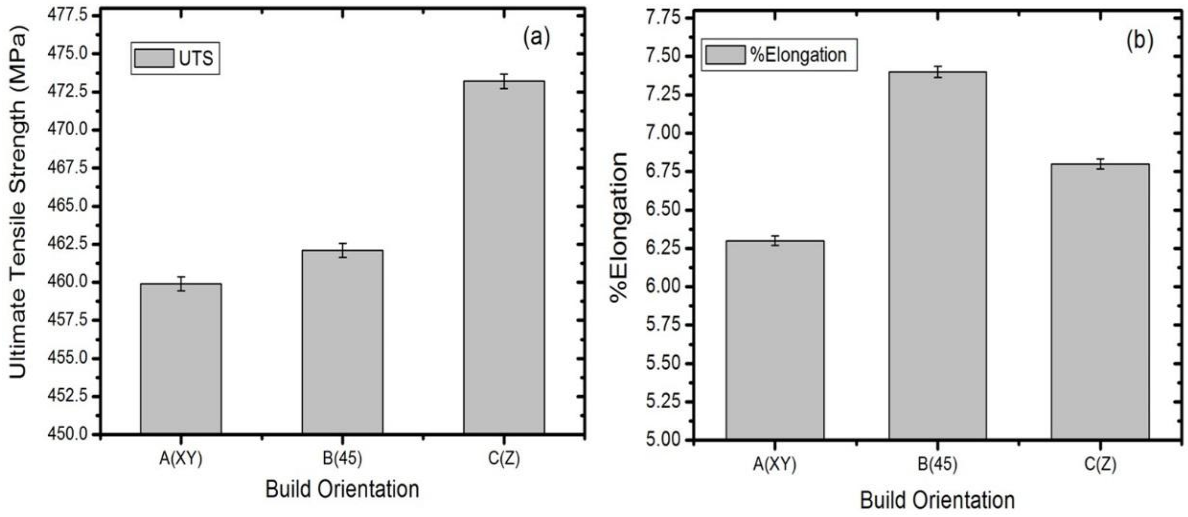

Figure 4. Tensile stress results of the SLM produced AlSi10Mg samples with build orientation and (a) ultimate tensile strength, and (b) %elongation.

4. Conclusions

The aim of this work was to demonstrate the effect of SLM build orientation on the microstructure, density, porosity and mechanical properties of AlSi10Mg samples. The results of this work substantiated anisotropy, which is the demonstration of different mechanical properties in different build orientations before thermal treatment. The samples varied in mechanical properties by built orientation with the Z orientations exhibiting the highest UTS though it also showed the highest levels of porosity from density measurements and microstructural analysis. Initially from density measurements, it was apparent that batch A was to be selected for further modification relatively to the rest of the samples, but with further tests for tensile strength, it was distinguished that batch B would be the best to be chosen practically to manufacture a part. Therefore, based on the obtained results, it can be concluded that the final application will determine the chosen build orientations as part of the process parameters in order to obtain the desired results. For instance, in applications that require ductile components, batch B will be ideal whereas for high strength, batch C is comparable to currently available literature values.

Acknowledgments

Metal Heart Additive Manufacturing, Tshwane University of Technology, Council for Scientific and Industrial Research (South Africa) is gratefully acknowledged. The authors would also like to thank National Laser Center (NLC) Metallurgical Laboratory and Material Science and Manufacturing Mechanical Testing Laboratory for sample preparation and characterization. The National Research Foundation Grant No. 114675 is acknowledged for conference funding. Acknowledgement also goes to the following individuals for their support, Mr. Thabo Lengopeng, Mr. Khoro Malabi, Mr Nana Arthur, Mr. Paul Lekoadi and Mr. Rendani Nemagovhani.

References

[1] I. Rosenthal, A. Stern, N. Frage, *Metallography, Microstructure, and Analysis*, **3** (2014) 448-453.
[2] P. Hanzl, M. Zetek, T. Bakša, T. Kroupa, *Procedia Engineering*, **100** (2015) 1405-1413.
[3] W. Li, S. Li, J. Liu, A. Zhang, Y. Zhou, Q. Wei, C. Yan, Y. Shi, *Materials Science and Engineering: A*, **663** (2016) 116-125.
[4] L. Portolés, O. Jordá, L. Jordá, A. Uriondo, M. Esperon-Miguez, S. Perinpanayagam, *Journal of Manufacturing Systems*, **41** (2016) 65-75.

[5] E. Gmbh, in: EOS (Ed.), 2014.
[6] E. Brandl, U. Heckenberger, V. Holzinger, D. Buchbinder, *Materials & Design*, **34** (2012) 159-169.
[7] I. Rosenthal, A. Stern, N. Frage, *Materials Science and Engineering: A*, **682** (2017) 509-517.
[8] L.P. Lam, D.Q. Zhang, Z.H. Liu, C.K. Chua, *Virtual and Physical Prototyping*, **10** (2015) 207-215.
[9] K. Kempen, L. Thijs, E. Yasa, M. Badrossamay, J.P. Kruth, in: Solid Free Form Fabrication Symposium, Texas, USA, 2011.
[10] M. Awd, J. Tenkamp, M. Hirtler, S. Siddique, M. Bambach, F. Walther, *Materials*, **11** (2017) 10.3390/ma11010017.
[11] K. Kempen, L. Thijs, J. Van Humbeeck, J.P. Kruth, *Physics Procedia*, **39** (2012) 439-446.
[12] I. Rosenthal, A. Stern, N. Frage, *Metallography Microstructure and Analysis*, **3** (2014) 448 - 453.
[13] N. Takata, H. Kodaira, A. Suzuki, M. Kobashi, *Materials Characterization*, (2017).
[14] E.G.-E. Systems, in: E. GmbH (Ed.), 2017.
[15] F. Trevisan, F. Calignano, M. Lorusso, J. Pakkanen, E. Ambrosio, M. Lombardi, M. Pavese, D. Manfredi, P. Fino, in: World Powder Metallurgy Congress 2016, Hamburg, Germany, 2016.